A comparison of DAE integrators in the context of benchmark problems for flexible multibody dynamics

Article *in* Journal of Mechanical Science and Technology · July 2015

DOI: 10.1007/s12206-015-0511-5

5 authors, including:

Peter Betsch
Karlsruhe Institute of Technology
171 PUBLICATIONS **2,707** CITATIONS
SEE PROFILE

Marlon Franke
Karlsruhe Institute of Technology
26 PUBLICATIONS **149** CITATIONS
SEE PROFILE

Yinping Yang
Beijing University of Technology
8 PUBLICATIONS **26** CITATIONS
SEE PROFILE

Alexander Janz
Karlsruhe Institute of Technology
15 PUBLICATIONS **72** CITATIONS
SEE PROFILE

Springer

KSME

Journal of Mechanical Science and Technology 29 (7) (2015) 2653~2661
www.springerlink.com/content/1738-494x(Print)/1976-3824(Online)
DOI 10.1007/s12206-015-0511-5

A comparison of DAE integrators in the context of benchmark problems for flexible multibody dynamics †

Peter Betsch*, Christian Becker, Marlon Franke, Yinping Yang and Alexander Janz

Institute of Mechanics, Karlsruhe Institute of Technology (KIT), Otto-Ammann-Platz 9, 76131 Karlsruhe, Germany

(Manuscript Received December 4, 2014; Revised March 20, 2015; Accepted March 20, 2015)

Abstract

In the present work a uniform framework for general flexible multibody dynamics is used to compare state-of-the-art DAE integrators in the context of benchmark problems. The multibody systems considered herein are comprised of rigid bodies, nonlinear beams and shells. The constitutive laws applied in the benchmark problems belong to the class of hyperelastic materials. To numerically integrate the uniform set of DAEs three alternative time-stepping schemes are applied: (i) an energy-momentum consistent method, (ii) a specific variational integrator and (iii) a generalized-α scheme.

Keywords: Differential-algebraic equations; Multibody systems; Nonlinear structural mechanics; Structure-preserving discretization; Time-stepping schemes

1. Introduction

A general description of flexible bodies belonging to a multibody system is based on Cosserat theories for shells, beams and points [1]. For example, the theory of Cosserat points comprises rigid body dynamics in terms of natural coordinates as a special case [2]. Similarly, geometrically exact models for beams and shells are covered by corresponding Cosserat theories. Using natural coordinates along with a structure-preserving discretization in space of flexible bodies yields a general framework for flexible multibody dynamics [3]. The motion of the corresponding constrained mechanical systems is governed by a uniform set of differential-algebraic equations (DAEs).

Over the last decade highly promising methods for the direct discretization of the DAEs related to constrained mechanical systems have been developed. Among others, these are: the generalized-α scheme [4, 5], variational integrators [6], and energy-momentum methods [7]. In particular, both generalized-α and energy-momentum schemes have been designed to meet the specific demands of discrete mechanical systems stemming from nonlinear structural mechanical formulations.

In the present work the aforementioned three alternative DAE integrators will be applied to challenging benchmark problems for flexible multibody systems. Of course, a specific integrator only qualifies for the demanding class of flexible multibody systems if it is capable of correctly reproducing the results of classical benchmarks for multibody systems, solely comprised of rigid bodies, such as Andrews' squeezer mechanism [8]. Similarly, discrete models for flexible bodies such as beam and shell finite elements should only be employed in a flexible multibody system if they correctly reproduce the results of benchmarks for the static analysis of large deformation problems.

Due to the intrinsic complexity of flexible multibody systems the design of appropriate benchmarks is itself a challenging task [9]. To be reproducible, a benchmark problem for flexible multibody dynamics should be as simple as possible. Still a large amount of data is typically required to set up the system.

Accordingly, web-based platforms, such as Ref. [10], are an important tool for the data exchange between researchers.

Of course, benchmark problems should be realistic from a physical point of view. This implies the specification of consistent initial conditions, clearly defining all of the state variables. Moreover, in many cases the incorporation of dissipative material behavior and joint-friction is important for the physical relevance of the model. We remark, however, that the present work is restricted to nondissipative flexible multibody systems.

An outline of the rest of the paper is as follows. In Sec. 2 we summarize the uniform computational framework applied in the present work for the simulation of flexible multibody dynamics. Concerning the numerical integration of the discrete equations of motion three alternative DAE integrators are used.

*Corresponding author. Tel.: +49 721 608 42072, Fax.: +49 721 608 47990
E-mail address: Peter.Betsch@kit.edu

† This paper was presented at the Joint Conference of the 3rd IMSD and the 7th ACMD, Busan, Korea, June, 2014. Recommended by Guest Editor Sung-Soo Kim and Jin Hwan Choi

Table 1. Parameters of the four-bar flexible mechanism.

Bar	AB	BC	CD
Length [m]	0.12	0.24	0.12
Young's modulus E [N/m²]	2.1e11	2.1e11	2.1e11
Poisson ratio ν	0.3	0.3	0.3
Normal stiffness EA [N]	4.e7	4.e6	4.e5
Bending stiffness EI [N/m²]	2.4e6	2.8e5	2.4e4
Torsion stiffness GJ [N/m²]	2.8e5	2.8e4	2.8e4
Shear stiffness GA [N]	2.e6	2.e5	2.e5
Mass per unit length [kg/m]	3.2	1.6	1.6
Section inertia about beam axis J_i [kgm]	2.4e-2	1.2e-2	1.2e-2
Section inertia about transverse axis I_i [kgm]	1.2e-2	6.e-3	6.e-3

In Secs. 3-5, these integrators are compared in the context of three benchmark problems for flexible multibody dynamics. Eventually, conclusions are drawn in Sec. 6.

2. Computational framework

To describe general flexible multibody systems we employ finite elements relying on nonlinear strain measures. Due to the frame-indifference of the underlying continuum models the present method is capable of correctly reproducing large deformations including finite rotations. The description of rigid bodies, geometrically exact beams and shells fits into the framework of associated Cosserat theories [1].

Typically these models give rise to a nonlinear configuration manifold. Instead of applying specific local parametrizations, our approach relies on the embedding of the configuration manifold in linear space. Consequently, we work with redundant coordinates and the motion of the discrete system is governed by DAEs. In particular, the present approach leads to a uniform set of DAEs for general multibody systems comprised of continuum bodies, beams, shells and rigid bodies. For more details we refer the interested reader to Refs. [2, 3, 11]. The uniform set of DAEs makes possible the application and direct comparison of alternative DAE integrators. In particular, in the present work we apply the following schemes:

- Energy-momentum consistent integrator (EM)
- Variational integrator (VI)
- Generalized-α time integration method (Gen-α).

Both the EM method and the VI scheme have been dealt with in detail in Ref. [12]. While the VI integrator has been developed in Ref. [6], the EM method forms an integral part of our previous works [2, 3, 11]. The Gen-α method applied in the present work relies on the developments in Ref. [5]. Early variants of the Gen-α method have been proposed in Refs. [13-15]. More recent developments are presented in Refs. [4, 16-18]. An extension of the Gen-α method to Lie groups has recently been proposed in Refs. [19, 20].

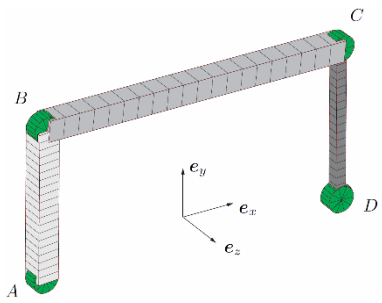

Fig. 1. Four-bar flexible mechanism: Reference configuration (Iso-perspective).

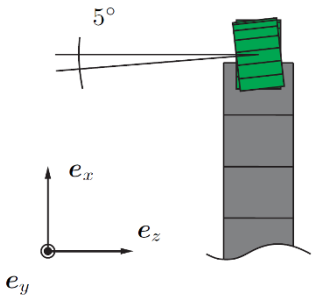

Fig. 2. Four-bar flexible mechanism: Misaligned hinge C (Top-perspective).

3. Four-bar flexible mechanism with a misaligned hinge

This problem shown in Fig. 1 has been originally proposed in Ref. [21, Sec. 10.2], see also the book [22] and the webpage [10]. We prefer a slight variant of the original problem proposed in Ref. [20, Sec. 7.3], where the misalignment of the revolute joint (at point C) is specified precisely and the rotation of the actuated joint (Point A) is prescribed instead of the actuating torque. The data used in the simulations is summarized in Table 1. The orientation of the misaligned hinge (C) is defined by an angle of 5°, measured positively about the y-axis (see Fig. 2). The angle θ_A of the revolute joint (A) is prescribed with a smooth acceleration phase between $t = t_0$ and $t = t_s$, followed by a constant speed phase according to

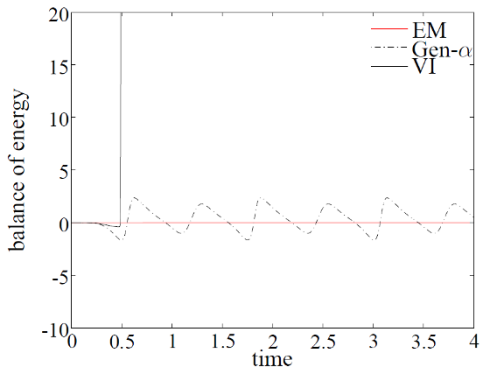

Fig. 3. Four-bar flexible mechanism: Balance of energy.

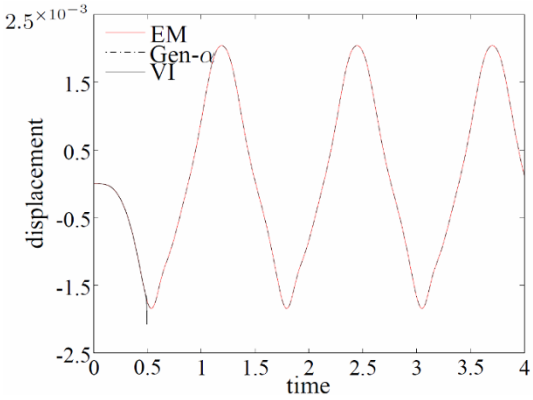

Fig. 4. Four-bar flexible mechanism: z-displacement at joint (C).

$$\theta_A(t)=\begin{cases}(\omega/ts)\left(t^2/2+(ts/(2\pi))^2\left(\cos(2\pi t/ts)-1\right)\right) & \text{for } t0\le t\le ts\\ \omega(t-ts/2) & \text{for } ts\le t\end{cases} \tag{1}$$

with $t_0 = 0$ s, $t_s = 0.5$ s and $\omega = -5$ rad/s. Note that the rotation takes place about the axis $-\mathbf{e}_z$. Each bar is discretized with ten 3-node (or quadratic) beam finite elements. Concerning the Gen-α method, the spectral radius at infinite frequency has been chosen to be $\rho_\infty = 0.9$. All subsequent numerical results have been calculated with a time step size of $h = 1\times10^{-3}$. In Fig. 3 the fulfillment of the balance law for energy is checked. While, as expected, the EM scheme perfectly obeys the balance law for energy, this is not the case for the Gen-α method. It can be further observed from Fig. 3 that the VI scheme shows an energy blow-up at $t \approx 0.45$ indicating a severe lack of numerical stability. Despite the lack of energy consistency, the Gen-α method exhibits numerical robustness and stability properties similar to the EM scheme.

Due to the misaligned joint, the four-bar linkage experiences out of plane displacements as depicted in Fig. 4. In addition to that, Fig. 5 gives an impression of the bending and torsion deformation triggered by the misaligned joint. Eventually, the motion of the four-bar linkage is illustrated in Fig. 6

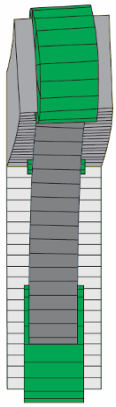

Fig. 5. Four-bar flexible mechanism: Deformed configuration at t = 0.48 (Front view).

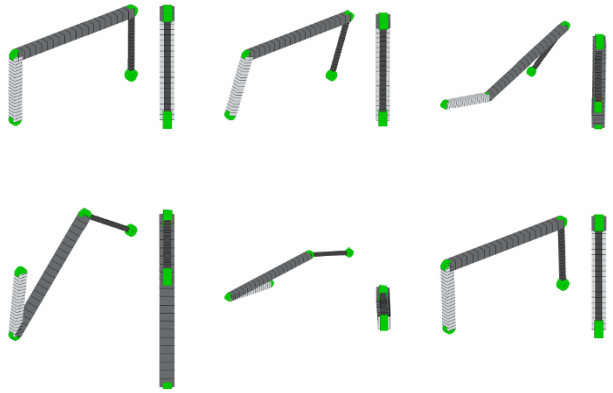

Fig. 6. Four-bar flexible mechanism: Snapshots of configurations at t ∈ {0, 0.3, 0.6, 0.9, 1.2, 1.5, ... } (Iso-perspective and front view).

with a sequence of subsequent snapshots.

4. Andrew's squeezer mechanism

The next problem can be considered a classical benchmark for multibody dynamics. According to Ref. [23, Sec. 3.6.9] this mechanism can be traced back to the PhD thesis by G.C. Andrews (1971). A detailed description of Andrews' squeezer mechanism can be found in the Multibody Systems Handbook [24], the book [25, Ch. VII.7] and the Technical Report [26]. Related numerical investigations have also been documented in Ref. [5, Sec 5.2].

The multibody system at hand consists of 7 rigid bodies interconnected by frictionless revolute joints (Fig. 7). The coordinates of the joints are given in Table 2. In addition to that, the inertia properties as well as the coordinates of the center of mass for all bodies are given in Table 3.

Moreover a spring with spring coefficient $c_0 = 4530$ N/m and unstretched length $l_0 = 0.07785$ m is connected to the present multibody system. The spring length in the initial configuration ($t_0 = 0$) is 0.05267 m.

The body-fixed frames are located in the center of mass of each body. The mechanism is driven by a motor located at

Table 2. Andrew's squeezer mechanism: Coordinates of the joints.

Joints	x [m]	y [m]
O	0	0
A	-0.06934	-0.00227
B	-0.03635	0.03273
C	0.01400	0.07200
D	-0.01047	0.02536
E	-0.03400	0.01646
F	-0.03163	-0.01562
G	0.00699	-0.00043
P	-0.02096	0.00130

Table 3. Andrew's squeezer mechanism: Inertia data and coordinates of the center of mass.

Link	Mass [kg]	Rotational inertia [kg·m^2]	x [m]	y [m]
K1	0.04325	$2.194\cdot10^{-6}$	$9.182\cdot10^{-4}$	$5.700\cdot10^{-5}$
K2	0.00365	$4.410\cdot10^{-7}$	$-4.491\cdot10^{-3}$	$2.788\cdot10^{-4}$
K3	0.02373	$5.255\cdot10^{-6}$	$1.874\cdot10^{-2}$	$2.048\cdot10^{-2}$
K4	0.00706	$5.667\cdot10^{-7}$	$-3.022\cdot10^{-2}$	$1.207\cdot10^{-2}$
K5	0.07050	$1.169\cdot10^{-5}$	$-5.324\cdot10^{-2}$	$1.663\cdot10^{-2}$
K6	0.00706	$5.667\cdot10^{-7}$	$-2.854\cdot10^{-2}$	$-1.072\cdot10^{-2}$
K7	0.05498	$1.912\cdot10^{-5}$	$-5.926\cdot10^{-2}$	$-1.060\cdot10^{-2}$

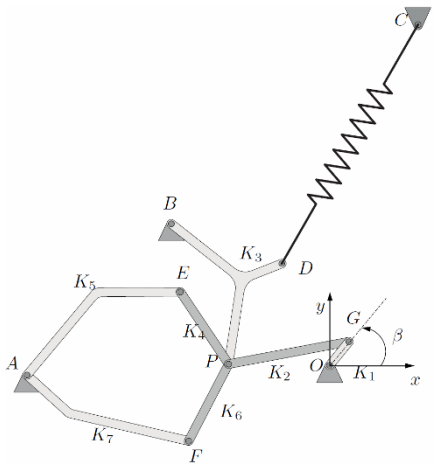

Fig. 7. Andrew's squeezer mechanism: Setup.

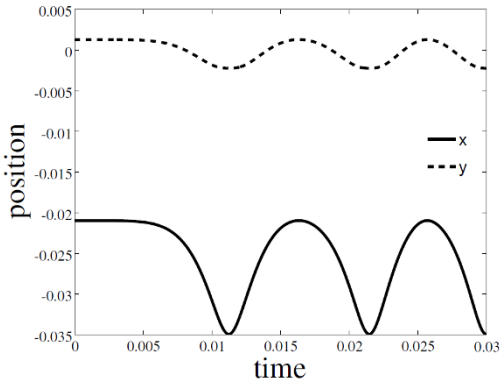

Fig. 8. Displacement of hinge (P).

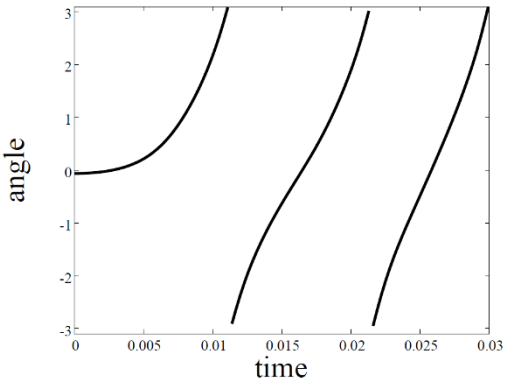

Fig. 9. Angle β [rad].

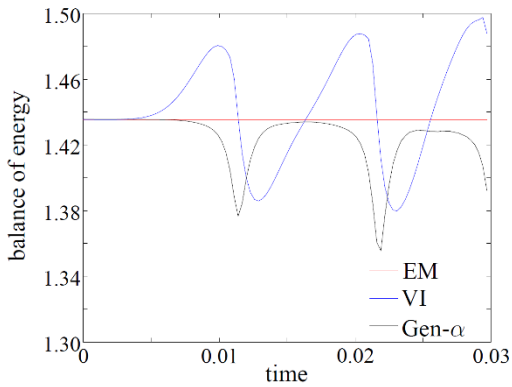

Fig. 10. Andrew's squeezer mechanism, $\Delta t = 3\cdot10^{-4}$ s.

point O. A constant torque M = 0.033 Nm is applied. In the initial configuration (t = 0) the mechanism is at rest. Obviously, the mechanism at hand has one degree of freedom. In the numerical simulations gravitation is not taken into account.

In Fig. 8 the two displacement components corresponding to joint (P) are plotted versus time. Similarly the angle β is plotted over time in Fig. 9. Again it can be observed from Fig. 10 that the EM scheme adheres to the balance law for energy, whereas both Gen-α and VI fail to satisfy this balance law. Of course, since Gen-α and VI are consistent, refinement of the time step yields an improved fulfillment of the balance of energy. This is shown in Fig. 11.

Altogether, for this classical multibody example, the overall performance of the three alternative integrators under investigation is very similar. In particular, the VI does not exhibit any numerical instability as in the last example. Fig. 12 shows the results for the Lagrange multiplier for the enforcement of the algebraic constraint associated with x direction of the revolute joint P (cf. Fig. 7). Due to the small time step $\Delta t = 3\cdot10^{-5}$ s the results of the three integrators under investigation are practically indistinguishable.

To illustrate the motion of the whole multibody system at hand several snapshots are plotted in Fig. 13.

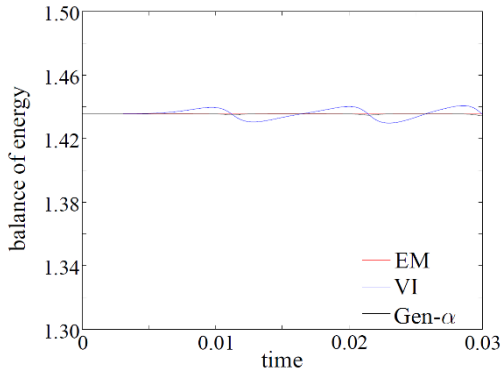

Fig. 11. Andrew's squeezer mechanism, $\Delta t = 3 \cdot 10^{-5}$ s.

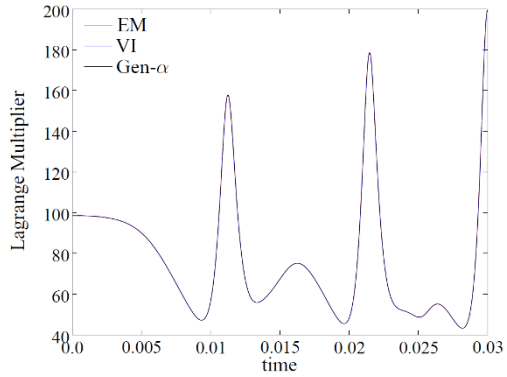

Fig. 12. Andrew's squeezer mechanism.

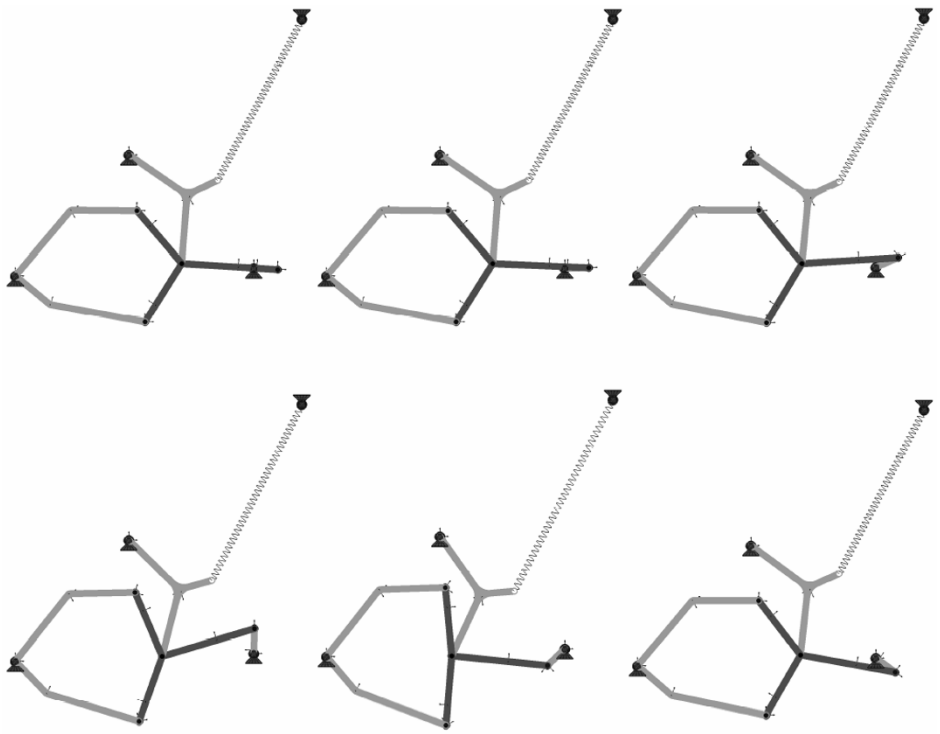

Fig. 13. Snapshots of configurations at t ∈ {0, 0.003, 0.006, 0.009, 0.012, 0.015, ...}.

5. Lateral buckling of a thin beam

The last numerical example deals with a flexible beam actuated by a crank mechanism (Fig. 14). This example is part of O. Bauchau's benchmark initiative [27]. Alternative variants of this problem can be found, for example, in Refs. [22, 28, 29].

The flexible beam (AB) is clamped at point A and connected to the link (CD) through a spherical joint in C. The connection (BC) between the beam and the spherical joint is assumed to be rigid and massless (see Fig. 15). The crank (DE) is on one side connected to the link at point D and on the other side attached to the ground (E) by means of revolute joints. The dimensions and properties of the present mechanism are summarized in Table 4, see also the webpage [10]. Both the link (CD) and the crank (DE) are modeled by flexible beams as well.

Due to the small offset (BC) between the beam (AB) and the crank mechanism, lateral buckling will occur when the crank mechanism pushes the beam up and a critical value of the transverse load is reached. The rotation of the crank joint in E about the negative $\mathbf{e}_y$-axis is prescribed as

$$\theta_E(t) = \begin{cases} \pi\left(1-\cos\left(\pi t / T\right)\right) & \text{for } t \le T \\ \pi & \text{for } t > T \,. \end{cases} \tag{2}$$

The slender beam (AB) has rectangular cross section (cf. Table 4) and can be modeled as shell as well. Accordingly, in our numerical investigations we compare the results of the

Table 4. Parameters of the lateral buckling mechanism.

Bar	AB	CD	DE
Length [m]	1	0.25	0.05
Height, width [m]	0.1, 0.01	-, -	-, -
Radius [m]	-	0.012	0.024
Young's modulus E [N/m^2]	73e9	73e9	73e9
Poisson ratio ν	0.3	0.3	0.3
Axial stiffness EA [N]	73e6	3.302e7	1.321e8
Bending stiffness EI_{22}, EI_{33} [Nm^2]	60830, 608.3	1189, 1189	19020, 19020
Shear stiffness K_{22}, K_{33} [N]	5.025e6, 2.34e7	1.081e7, 1.081e7	4.322e7, 4.322e7
Torsion stiffness GJ [Nm²]	877.2	914.5	14630
Mass per unit length [kg/m]	2.68	1.212	4.85
Section inertia I_2 [kgm]	2233e-6	43.65e-6	698.3e-6
Section inertia I_3 [kgm]	22.33e-6	43.65e-6	698.3e-6

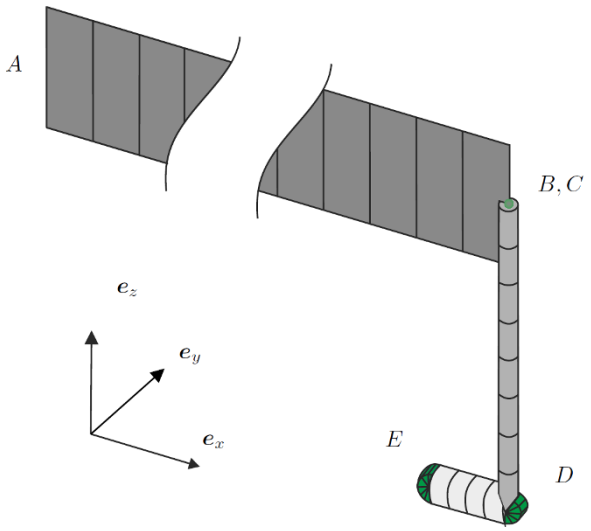

Fig. 14. Iso view: Reference configuration of the mechanism. Here, the slender beam (AB) is depicted with the mid-surface of the shell model.

beam model with those of the corresponding shell model. To this end we apply the geometrically exact shell formulation described in Refs. [11, 3].

The beam model of the slender beam (AB) is discretized with 16 quadratic beam finite elements, while the shell model is discretized with 32×8 bi-linear shell finite elements. The dynamic simulation is performed for 500 time steps of size $\Delta t = 1 \cdot 10^{-3}$.

Fig. 16 depicts the displacement at the midspan of the slender beam (AB). In the case of the shell model this point coincides with the mid-point on the mid-surface. It can be observed from Fig. 16 that the results of both the beam and the shell model are in good agreement.

Since the prescribed rotation angle of the crank stays constant for t > T = 0.4, the total energy of the mechanical system

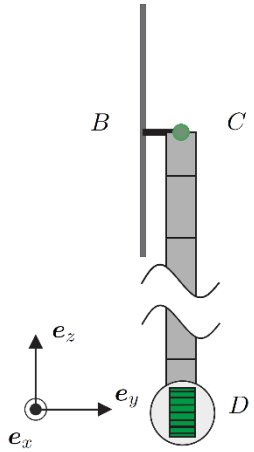

Fig. 15. Top view: Initial imperfection (BC).

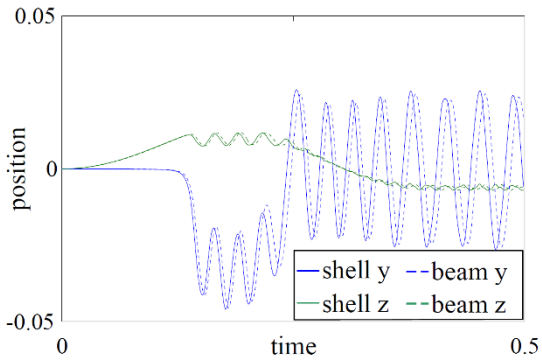

Fig. 16. Displacement of the shell (AB) and beam (AB) at midspan.

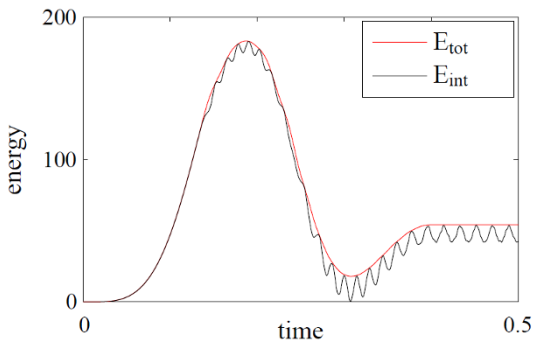

Fig. 17. Energy versus time of the shell model.

at hand is a conserved quantity. This conservation property is exactly reproduced by the EM scheme, as can be seen from Fig. 17. When the buckling load is reached, the slender beam (AB) snaps laterally and starts to oscillate. Correspondingly, oscillations in the internal energy E_{int} due to elastic deformations can be observed from Fig. 17.

As in the first example dealing with a flexible multibody example (Sec. 3) the Gen-α method performs practically as good as the EM scheme. Again the VI turns out to be prone to numerical instability and is not competitive to the other two

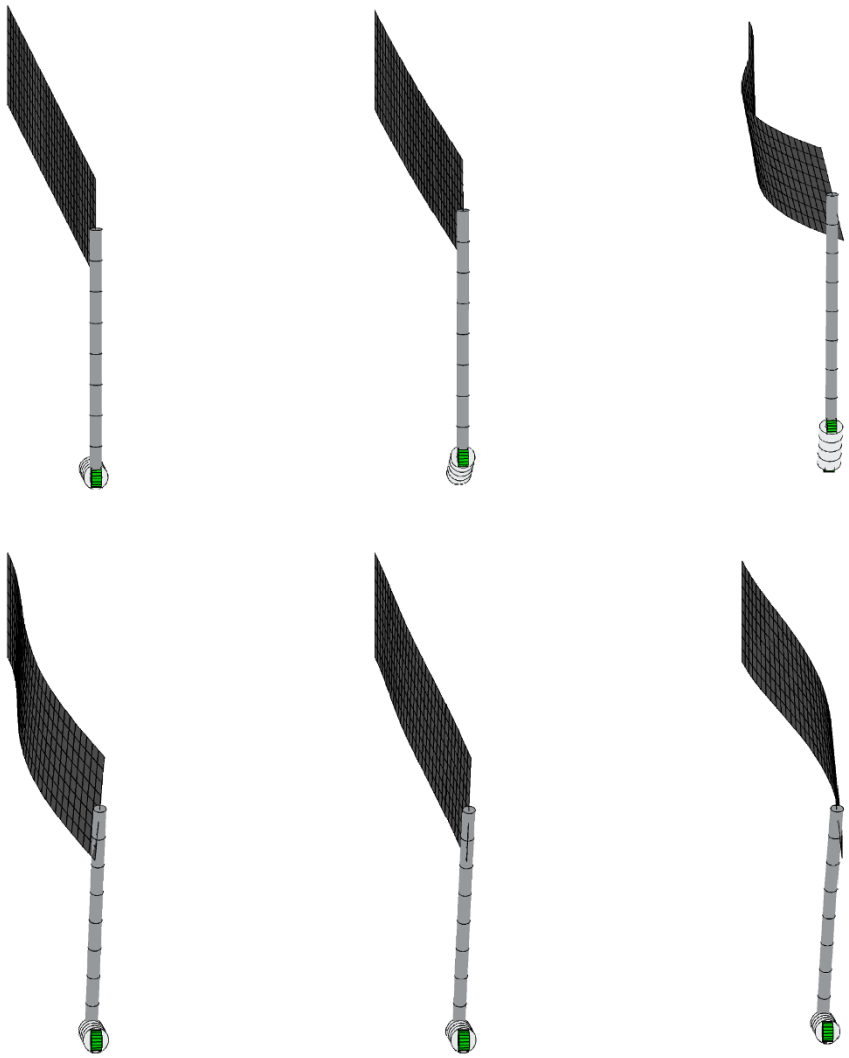

Fig. 18. Snapshots of configurations at t ∈ { 0, 0.1, 0.15, 0.39, 0.4, 0.41}.

schemes under investigation.

Fig. 18 contains a series of snapshots illustrating the violent lateral motion of the shell induced by the lateral buckling.

6. Conclusion

Three alternative DAE integrators were applied to three benchmark problems for multibody dynamics. The DAEs governing the motion of the multibody systems were generated by the method developed previously in Refs. [3, 11, 30]. It was shown that all three integrators under consideration perform well when applied to classical multibody systems in which all of the bodies are assumed to be rigid. In the case of flexible multibody dynamics both the EM scheme and the Gen-α method exhibit superior stability and robustness properties. In contrast to that the VI shows a tendency towards numerical instabilities if nonlinear beams or shells are part of the flexible multibody system. This observation is in line with previous results documented in Ref. [12].

Acknowledgment

Support for this research was provided by the Deutsche Forschungsgemeinschaft (DFG) under Grant BE 2285/9-1. This support is gratefully acknowledged.

References

[1] M. B. Rubin, Cosserat theories: Shells, rods and points, *Solid Mechanics and its Applications*, Kluwer Academic Publishers, 79 (2000).

[2] P. Betsch and N. Sänger, On the consistent formulation of torques in a rotationless framework for multibody dynamics, *Computers & Structures*, 127 (2013) 29-38.

[3] P. Betsch and N. Sänger, A nonlinear finite element framework for flexible multibody dynamics: Rotationless formulation and energy-momentum conserving discretization, In Carlo L. Bottasso, editor, Multibody Dynamics: Computational Methods and Applications, *Computational Methods in Applied Sciences*, Springer-Verlag, 12 (2009) 119-141.

[4] D. Negrut, R. Rampalli, G. Ottarsson and A. Sajdak, On an implementation of the Hilber-Hughes-Taylor method in the context of index 3 differential-algebraic equations of multibody dynamics (DETC2005-85096), *J. Comput. Nonlinear Dynam*., 2 (2007) 73-85.

[5] M. Arnold and O. Brüls, Convergence of the generalized-α scheme for constrained mechanical systems, *Multibody System Dynamics*, 18 (2) (2007) 185-202.

[6] S. Leyendecker, J. E. Marsden and M. Ortiz. Variational integrators for constrained dynamical systems, Z. Angew, *Math. Mech. (ZAMM)*, 88 (9) (2008) 677-708.

[7] S. Leyendecker, P. Betsch and P. Steinmann, The discrete null space method for the energy consistent integration of constrained mechanical systems, Part III: Flexible multibody dynamics, *Multibody System Dynamics*, 19 (1-2) (2008) 45-72.

[8] M. González, D. Dopico, U. Lugrís and J. Cuadrado, A benchmarking system for MBS simulation software: Problem standardization and performance measurement, *Multibody System Dynamics*, 16 (2) (2006) 179-190.

[9] M. Valášek, Z. Šika and T. Vampola, Criteria of benchmark selection for efficient flexible multibody system formalisms, *Applied and Computational Mechanics*, 1 (2007) 351-356.

[10] *http://www.dymoresolutions.com/Benchmarks/Benchmarks.html*.

[11] P. Betsch and N. Sänger, On the use of geometrically exact shells in a conserving framework for flexible multibody dynamics, *Comput. Methods Appl. Mech. Engrg*., 198 (2009) 1609-1630.

[12] P. Betsch, C. Hesch, N. Sänger and S. Uhlar, Variational integrators and energy-momentum schemes for flexible multibody dynamics, *J. Comput. Nonlinear Dynam*., 5 (3) (2010) 031001/1-11.

[13] A. Cardona and M. Géradin, Time integration of the equations of motion in mechanism analysis, *Computers & Structures*, 33 (3) (1989) 801-820.

[14] A. Cardona and M. Géradin, Numerical integration of second order differential-algebraic systems in flexible mechanism dynamics, aditted by M.S. Pereira and J.A.C. Ambrósio, *Computer-Aided Analysis of Rigid and Flexible Mechanical Systems*, *NATO-ASI Series E: Applied Sciences*, Kluwer Academic Publishers, 268 (1994) 501-529.

[15] J. Yen, L. Petzold and S. Raha, A time integration algorithm for flexible mechanism dynamics: The DAE α-method, *Comput. Methods Appl. Mech. Engrg*., 158 (3-4) (1998) 341-355.

[16] C. Lunk and B. Simeon, Solving constrained mechanical systems by the family of Newmark and α-methods, Z. Angew, *Math. Mech. (ZAMM)*, 86 (10) (2006) 772-784.

[17] L. O. Jay and D. Negrut, Extensions of the HHT-α method to differential-algebraic equations in mechanics, *Electronic Transactions on Numerical Analysis*, 26 (2007) 190-208.

[18] D. Negrut, L. O. Jay and N. Khude, A discussion of low-order numerical integration formulas for rigid and flexible multibody dynamics, *Journal of Computational and Nonlinear Dynamics*, 4 (2) (2009) 021008/1-11.

[19] O. Brüls and A. Cardona, On the use of Lie group time integrators in multibody dynamics, *J. Comput. Nonlinear Dynam*., 5 (3) (2010) 031002/1-031002/13.

[20] O. Brüls, A. Cardona and M. Arnold, Lie group generalized-α time integration of constrained flexible multibody systems, *Mechanism and Machine Theory*, 48 (1) (2012) 121-137.

[21] O. A. Bauchau and C. L. Bottass, On the design of energy preserving and decaying schemes for flexible, nonlinear multi-body systems, *Comput. Methods Appl. Mech. Engrg*., 169 (1-2) (1999) 61-799.

[22] O. A. Bauchau, Flexible multibody dynamics, *Solid Mechanics and its Applications*, Springer-Verlag, 176 (2011).

[23] J. von Schwerin, *Multibody System SIMulation*, Springer-Verlag (1999).

[24] W. O. Schiehlen, Editor, *Multibody systems handbook*, Springer-Verlag (1990).

[25] E. Hairer and G. Wanner, *Solving ordinary differential equations II: Stiff and differential-algebraic problems*, Springer-Verlag (1991).

[26] N. Khude and D. Negrut, A MATLAB implementation of the seven-body mechanism for implicit integration of the constrained equations of motion, *Technical Report TR-2007-07*, Simulation-Based Engineering Laboratory, The University of Wisconsin-Madison (2007).

[27] O. A. Bauchau, G. Wu, P. Betsch, A. Cardona, J. Gerstmayr, B. Jonker, P. Masarati and V. Sonneville, Validation of flexible multibody dynamics beam formulations using benchmark problems, *Proceedings of the 3rd Joint International Conference on Multibody System Dynamics and the 7th Asian Conference on Multibody Dynamics (IMSD-ACMD)*, Busan, Korea, 30 June 30 - 3 July (2014).

[28] O. A. Bauchau, J. -Y. Choi and C. L. Bottasso, On the modeling of shells in multibody dynamics, *Multibody System Dynamics*, 8 (2002) 459-489.

[29] O. A. Bauchau, C. L. Bottasso and L. Trainelli, Robust integration schemes for flexible multibody systems, *Comput. Methods Appl. Mech. Engrg*., 192 (3-4) (2003) 395-420.

[30] P. Betsch and P. Steinmann, A DAE approach to flexible multibody dynamics, *Multibody System Dynamics*, 8 (2002) 367-391.

Peter Betsch received his Diploma degree in Aerospace Engineering from the University of Stuttgart, Germany in 1991, his Ph.D. degree in computational mechanics from the University of Hanover, Germany in 1996, and his venia legendi (Habilitation) in mechanics from the University of Kaiserslautern, Germany in 2002. During 2003-2013 he was a Professor of Computational Mechanics at the University of Siegen, Germany. Since 2013 he has been a Professor of Mechanics at the Karlsruhe Institute of Technology, Germany.

Christian Becker received his diploma degree in Mechanical Engineering from the University of Siegen, Germany in 2011. He is a Ph.D. candidate at the Karlsruhe Institute of Technology, Germany. His research interests include multibody dynamics, structure-preserving time integration and optimal control.

Marlon Franke studied Mechanical Engineering at the University of Siegen, Germany and received his Diploma degree in 2009. In 2014 he received his Ph.D. degree from the Karlsruhe Institute of Technology (KIT), Germany at the Department of Civil Engineering, Geo- and Environmental Sciences. Currently, he holds a postdoc position at the KIT. His main research interest includes computational continuum mechanics with special focus on numerical discretization techniques with respect to time and space. Areas of applications are contact (Thermo) mechanics and most recently the combination with modern phase-field crack propagation approaches.

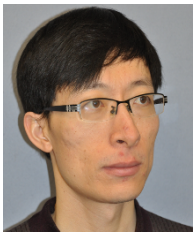

Yinping Yang studied Civil Engineering in China University of Mining and Technology and graduated with a Bachelor's degree. In Germany he studied Mechanical Engineering in University of Duisburg - Essen and graduated with a Bachelor's and a Master's degree. He is now a research associate and also a Ph.D. candidate in Karlsruhe Institute of Technology. His research interest is "Numerical Methods in the inverse Dynamics of Mechanical Systems".

Alexander Janz studied Mechanical Engineering at the University of Siegen, Germany and received his Bachelor degree in 2012 and his Master degree in 2014. Currently he is working as research associate at the Karlsruhe Institute of Technology (KIT), Germany at the Department of Civil Engineering, Geo- and Environmental Sciences. His main research focuses on structure-preserving integration with mixed finite elements.